1

Galaxy clusters as probes of cosmology and astrophysics

AUGUST E. EVRARD
Departments of Physics and Astronomy, Michigan Center for Theoretical Physics, University of Michigan

Abstract

Clusters of galaxies emerge as nodes in the gravitationally evolving cosmic web of dark matter and baryons that defines the large-scale structure of the Universe. X-ray and optical observations offer plentiful evidence of clusters' dynamical youth, yet bulk measures derived from these observations are tightly correlated, indicating a high degree of structural regularity that makes the population an attractive probe of cosmology. Accurate constraints on cosmological parameters require a precise and unbiased model relating observables to total mass, as well as a statistical characterization of the massive halo population within a given cosmology. In this contribution, I focus on the latter by providing evidence from simulations for $\mathcal{O}(10\%)$ calibration of the space density as a function of mass and for $\mathcal{O}(1\%)$ calibration of the dark matter virial relation. Matching the observed space density as a function of X-ray temperature for a ΛCDM world model is presented as an example of astrophysical/cosmological confusion. The resulting constraint $\beta\sigma_8{}^{-5/3} = (1.10 \pm 0.07)$ combines β, the ratio of specific energies in dark matter and intracluster gas, with σ_8, the normalization of the mass fluctuation spectrum. Disentangling astrophysical and cosmological factors for upcoming large statistical surveys is the main challenge in the quest to use galaxy clusters as sensitive probes of dark matter and dark energy.

1.1 Introduction

Cosmology is now a data-rich subject, with empirical support from at least four independent channels: the cosmic microwave background (CMB) radiation, light element nucleosynthesis, Type Ia supernovae, and large-scale cosmic structure. The latest CMB observations from the *Wilkinson Microwave Anisotropy Probe* (*WMAP*; Bennett et al. 2003) and ground-based experiments have revealed the series of acoustic peaks expected in an inflationary, hot Big Bang picture (Scott, Silk, & White 1995) and spotlight a fundamentally unexpected model containing roughly two-thirds vacuum or dark energy, one-third dark matter, and about four percent ordinary (baryonic) matter (Spergel et al. 2003). The nature of the principal dark components remains a mystery.

The ornery energy of Fritz Zwicky, though unlikely to dominate the Universe, is nonetheless involved in all this. Zwicky's revelation of dark matter in the Coma cluster (Zwicky 1933, 1937) established the roots of the modern era, and it is fitting to recognize his seminal contributions at this centennial event of the Carnegie Observatories. The problem of *missing mass*, as it was then known, derived from the humble virial theorem, helped to spark the

Table 1.1. *Mass Hierarchy in the Coma Cluster*

Component	$M(< 1.5\,h^{-1}$ Mpc) $(M_\odot)$	$M/M_{\rm vis}$
Total[a]	$1.3 \pm 0.3 \times 10^{15}\ h_{70}^{-1}$	9.0 ± 2.5
Intracluster gas	$1.3 \pm 0.2 \times 10^{14}\ h_{70}^{-5/2}$	0.90 ± 0.02
Galaxies	$1.4 \pm 0.3 \times 10^{13}\ h_{70}^{-1}$	0.10 ± 0.03

[a]Estimated from gas dynamic simulations.

now vast and complex hunt at large collider experiments and underground laboratories for the particle constituent of dark matter.

A half-century after Zwicky's study, advances in X-ray astronomy revealed the full mass hierarchy within clusters: galaxies are outweighed by an encompassing hot intracluster medium (ICM), and the combined visible mass remains a minority of the total. High-throughput spectroscopy of the ICM established its nearly isothermal nature, and high-resolution imaging from the *ROSAT* mission (Briel, Henry, & Böhringer 1992) enabled accurate estimates of ICM masses as well as estimates of total masses, under a hydrostatic equilibrium assumption, which confirmed, within $\sim 30\%$ statistical errors, the optical virial estimates of Dressler (1978) and many others (see Girardi et al. 2000). Estimates of the mass hierarchy for the Coma cluster (White et al. 1993) are listed in Table 1.1 for a Hubble constant $H_0 = 70\,h_{70}$ km s^{-1} Mpc^{-1}.

Why was galaxy formation in Coma so inefficient? To what extent is the environment within Coma representative of the state of clusters in general? Or of the Universe as a whole? Answers to many of these questions are now becoming available from increasingly large statistical surveys of galaxies and clusters, along with detailed investigation of individual clusters using 8 m-class optical telescopes. Papers presented at this meeting offer many excellent examples of both such approaches.

On the theory side, modeling the development of galaxies and the ICM within a cosmological framework of hierarchical clustering poses a formidable task. Although the physical processes—gravity, heating by shocks, cooling and (especially in low-density regions) heating by radiation, magnetic fields, conduction, turbulent mixing, etc.—are now firmly in hand, the complex, nonlinear interactions that govern their time evolution are analytically intractable, even for highly simplified geometries. Computational solutions are progressing (Kauffman et al. 1999; Somerville & Primack 1999; Cole et al. 2000), but the accuracy of solutions is limited by uncertainties associated with the "mesoscopic" processes involved in stellar birth, evolution, and death. The role of central black holes/active galactic nuclei on the galaxy/ICM interaction is only beginning to be explored (cf. Brüggen & Kaiser 2002).

Such modeling uncertainties are a cause for concern to cosmologists, since biased parameter estimates will result from application of an incorrect astrophysical model. Let $\mathcal{C}$ represent the vector of cosmological parameters (clustered mass density $\Omega_{\rm m}$, baryon mass density $\Omega_{\rm b}$, vacuum energy density Ω_Λ or dark energy $\Omega_{\rm DE}$, spectrum normalization σ_8, etc.) and let $\mathcal{R}$ represent a set of observations from a cluster survey. Then Bayes' theorem makes clear that identifying the most likely cosmology is dependent on knowing precisely how likely are the observations within that world model:

$$p(\mathcal{C} \mid \mathcal{R}) \propto p(\mathcal{R} \mid \mathcal{C})\, p_{\rm prior}(\mathcal{C}). \tag{1.1}$$

For the CMB, the relevant likelihoods $p(\mathcal{R} \mid \mathcal{C})$ are calculable to high accuracy with codes such as CMBFAST (Seljak & Zaldarriaga 1996). For Type Ia supernovae, only the luminosity distance $d_L(z)$ is needed to compute the apparent brightness of standard candles as a function of redshift (although proving the standard candle nature is challenging). For galaxy clusters and most other large-scale structure signatures, nonlinear dynamics and astrophysical uncertainties complicate the computation of the observable likelihood $p(\mathcal{R} \mid \mathcal{C})$.

There are computational and empirical reasons to suspect that the problem, though complex, is still tractable. Tight correlations, such as that between ICM mass $M_{\rm ICM}$ and X-ray temperature $T_{\rm X}$ (Mohr, Mathiesen, & Evrard 1999), are observed among intrinsic properties of local clusters. Simulated clusters follow narrow scaling relations (Evrard 1989; Navarro, Frenk, & White 1995, hereafter NFW; Evrard, Metzler, & Navarro 1996; Bryan & Norman 1998). These findings motivate a basic framework in which clusters are essentially a one-parameter family ordered by a size parameter, typically taken to be the total mass M. (Exactly how mass is defined is a detail discussed below.) Tight scaling relations between M and $T_{\rm X}$ reflect virial equilibrium, while retention of the cosmic baryon fraction and inefficient cooling/star formation within cluster environments lead to a strong correlation $M_{\rm ICM} \sim (\Omega_{\rm b}/\Omega_{\rm m}) f_{\rm hot} M$, with $f_{\rm hot}$ the fraction of baryons not processed into cold gas or stars.

In this paper, I take the perspective of separating the problem into two, quasi-independent pieces. For a given cosmology, the question of computing the likelihood of an observable, say the expected number of clusters with temperate T at redshift z, can be split into two parts, namely

- How many clusters of mass M exist in this cosmology at redshift z?
- What is the likelihood that a cluster of mass M at redshift z will have temperature T?

In general, the answer to the second question will require an astrophysical model defined by some set of parameters $\mathcal{A}$. For example, varying the efficiency of supernova or active galactic nuclei heating will affect the detailed form of the joint likelihood $p(M, T)$ at a particular epoch.

Under this separable assumption, the likelihood of forming a cluster of temperature T at redshift z will be a convolution

$$p(T, z \,|\, \mathcal{C}, \mathcal{A}) = \frac{\int dM\; p(M, z \,|\, \mathcal{C})\; p(T \,|\, M, z, \mathcal{A})}{\int dM\; p(M, z \,|\, \mathcal{C})}, \tag{1.2}$$

where $p(M, z \,|\, \mathcal{C})$ gives the likelihood that a cluster of mass M exists at redshift z in cosmology $\mathcal{C}$ and $p(T \,|\, M, z, \mathcal{A})$ gives the likelihood that such a cluster has temperature T for the particular astrophysical model $\mathcal{A}$.

In § 1.2, after briefly reviewing the framework of nonlinear structure formation, I present recent calibrations of the cluster space density by large simulations and show that this problem, modulo some inherent arbitrariness in assigning mass to halos, is now on quite firm footing. In § 1.3, the virial relation linking mass to ICM temperature is discussed and discrepancies between computational and empirical approaches are noted. This motivates a "back-door" approach to calibrating the mass scale of the cluster population that stems from very precise determination of the dark matter virial relation discussed in § 1.4. Implications emerge in § 1.5, where the observed cluster space density as a function of temperature forges a link between σ_8 (a cosmological parameter) and the ratio of cluster component energies

β (a purely astrophysical parameter). Unless sources of substantial systematic error can be identified, the low normalization $\sigma_8 \approx 0.7-0.8$ inferred from *WMAP* analysis will require significantly more heating of the ICM plasma than is provided by gravitational collapse alone. A concluding discussion is provided in § 1.6.

1.2 Clusters as Dark Matter Potential Wells

An early inflationary period in the history of the Universe is thought to seed the Universe with fluctuations in energy density (Kolb & Turner 1990). Depending on the chosen scenario, the spectrum of primordial density fluctuations can differ from a power law, and a general expression is a form with a running spectral index:

$$P_{\rm prim}(k) \;=\; P(k_0)\left(\frac{k}{k_0}\right)^{n_s(k)}, \tag{1.3}$$

where $n_s(k) = n_s(k_0) + dn_s/\mathrm{d}\ln k\,\ln(k/k_0)$. Recent analysis of *WMAP* thermal fluctuations combined with 2dF galaxy and Lyα forest power spectrum estimates suggest, at the 2σ level, a nonzero value for the spectral index derivative $dn_s/\mathrm{d}\ln k = -0.031^{+0.016}_{-0.017}$ (Spergel et al. 2003).

During the pre-recombination era, when fluctuation amplitudes are small and a linear treatment of independent wavemodes is valid, the primordial matter perturbations undergo stagnant growth on small scales and (for warm/hot components) strong damping due to free-streaming. The net result of such physics, which is particularly sensitive to the matter density $\Omega_{\rm m}$ and the baryon fraction $\Omega_{\rm b}/\Omega_{\rm m}$, is summarized by a transfer function $T(k)$ that defines the post-recombination power spectrum $P_{\rm rec}(k) \equiv T^2(k)P_{\rm prim}(k)$ (Bond & Efstathiou 1984).

As discussed below, the mass dependence of the cluster space density is sensitive to the logarithmic slope of the linear, post-recombination spectrum $n_{\rm eff} = \mathrm{d}\ln P_{\rm rec}(k)/\mathrm{d}\ln k$ on $\sim 10\,h^{-1}$ Mpc scales. A statistically precise measurement of $n_{\rm eff}(k)$ can be sought using upcoming large cluster samples, after systematic selection and projection effects are addressed and understood.

1.2.1 Nonlinear Gravitational Condensation

In the linear regime, the growth rate of the fluctuation amplitude at any wavenumber is controlled by a function $D(a)$, the form of which is determined by the mix of matter and energy components in the Universe (Peebles 1980; Carroll, Press, & Turner 1992). As linearized wave amplitudes δ approach unity, mode coupling becomes important, and the linear treatment must be extended to second and higher order (Bernadeau et al. 2002). Comparison with N-body simulations confirm the validity of calculations to tenth order and higher (Szapudi et al. 2000), but precise solution of the deeply nonlinear ($\delta \gtrsim 10^2$) evolution of the matter density and velocity fields is exclusively achieved by numerical simulation (Bertschinger 1998).

Simulations of large comoving volumes show that, as mode-coupling strengthens, the density field develops the texture of a "cosmic web" (Bond, Kofman, & Pogosian 1996), an example of which is shown in Figure 1.1. Filaments and walls surround lower density voids and bound ellipsoidal structures—the halos/clusters housing astrophysical objects—develop through gravitational collapse, with the largest and rarest clusters forming at nodes defined by major filament intersections. As discussed below, the spectrum of halos sizes can be derived analytically from $P_{\rm rec}(k)$ under spherical or ellipsoidal evolution approximations. For

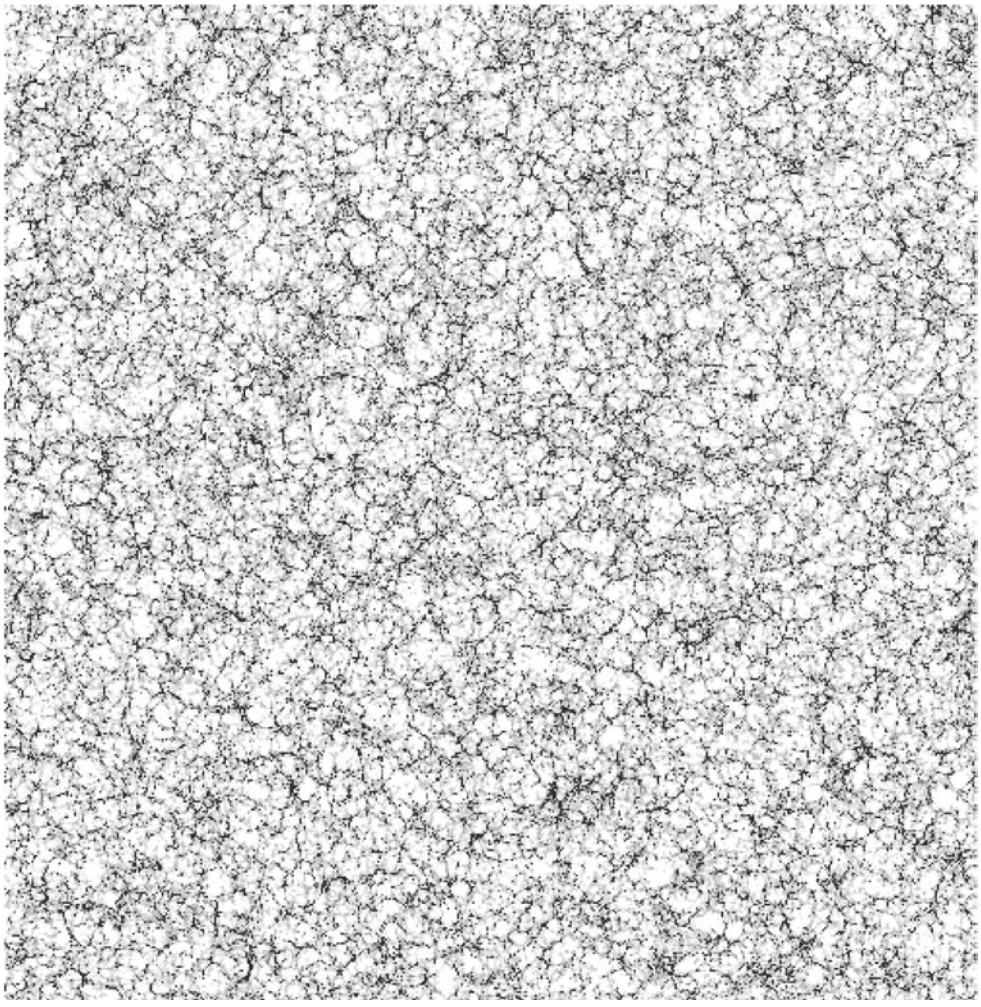

Fig. 1.1. Large-scale structure of cold dark matter in a Hubble Length ($3000\,h^{-1}$ Mpc) slice through a simulated ΛCDM Universe at $z = 0$ (Evrard et al. 2002). The slice thickness with $30\,h^{-1}$ Mpc and the greyscale show regions with above-average density smoothed on a $10^{13}\,h^{-1}M_{\odot}$ scale.

effectively power-law spectra, the characteristic mass scale M_* of the distribution evolves in redshift according to $M_*(a) \propto [D(a)]^{6/(n_{\rm eff}+3)}$ (Kaiser 1986), and this feature is the basis for deducing a low matter density Universe from the sky surface density of massive clusters at $z \approx 0.5-1$ (Bahcall & Fan 1998; Donahue et al. 1998; Borgani et al. 2001).

Since both the Gaussian random initial conditions and the process of gravitational amplification have no sharp intrinsic scales, clusters do not develop obvious physical boundaries. Instead, a roughly hydrostatic and dynamically older core connects seamlessly to an infall region fed by material drawn mainly from the embedding filaments. Accretion of small halos occurs nearly continuously up to the present, and major mergers that cause significant phase space rearrangement happen stochastically every few dynamical times. Due to this

complexity, a unique definition of cluster mass is hard to justify. Instead, a few, quite similar measures are in common use (Lacey & Cole 1994; White 2001, and references therein), each defined by a threshold density that attempts to separate the quasi-equilibrium, or "virialized", cluster interior from its surrounding, infalling streams.

One way to address the mass ambiguity is to consider the relative merits of different measures. What "added value" does each bring to descriptive analysis of the cluster population? As shown below, it appears that masses set by thresholds defined relative to the *mean* matter density $\rho_{\rm m}(a)$ are convenient for counting clusters, while those defined relative to the critical density $\rho_{\rm c}(a)$ are advantageous for addressing internal structure issues such as the virial relation linking mass to dark matter velocity dispersion or ICM thermal temperature.

In spherical models of perturbation evolution (Gunn & Gott 1972; Bertschinger 1985; Lokas & Hoffmann 2000), a cluster develops from a local peak in the linear density field. Peaks in Gaussian random fields exist on a wide range of scales, so to select those at a particular scale $M \propto R^3$ it is useful to smooth the continuous density field $\rho(x)$ with a spatial filter $W(|x'-x|/R)$. The variance in the smoothed density field is

$$\sigma^2(M) \;=\; \frac{1}{(2\pi)^3}\int d^3k\, P_{\rm rec}(k)\,\hat{W}^2(kR), \tag{1.4}$$

where $\hat{W}(kR)$ is the Fourier transform of the spatial filter function. The use of a spherical Heaviside, or "top-hat," function [$W(r/R)\equiv 1$ for $r/R \le 1$ and 0 otherwise] with comoving scale $8\,h^{-1}$ Mpc defines a conventional measure of the present, linearly evolved power spectrum amplitude $\sigma_8 \equiv \sigma(M_8)$, with $M_8 = 1.785(\Omega_{\rm m}/0.3)\times 10^{14}\,h^{-1}M_\odot$. The probability density function (PDF) of the filtered density field is Gaussian normal in the variable $\nu \equiv \delta/\sigma(M)$.

1.2.2 The Cluster Space Density

Counting the number of clusters as a function of size is currently an inexact exercise for observers and theorists alike. In the sky, optical/infrared catalogs can be searched for galaxy concentrations in redshift/color space (Bahcall et al. 2003; Nichol 2004). Detection of the ICM via its X-ray emission (Rosati, Borgani, & Norman 2002) or its spectral distortion of the microwave background radiation (Carlstrom, Holder, & Reese 2002) is another means of cluster identification. Although the observable signatures are strongly correlated (to first order, via the ever-useful "bigger is bigger" maxim), the scaling relations linking pairs of observables display typically tens of percent intrinsic scatter (Borgani et al. 1999; Mohr et al. 1999; Sanderson et al. 2003), and each measure is subject to different sources of systematic and random errors.

The upshot is that an X-ray temperature-limited sample of clusters will differ somewhat from an optical richness-limited sample, and both will differ to some degree with an Sunyaev-Zel'dovich-limited set of clusters. Given enough signal-to-noise ratio, the most massive clusters will be identified by any method, but differences in how projected signals add, along with intrinsic scatter among observables, will, at the minimum reorder, and more likely reorder and blend a set of objects detected at even high signal-to-noise ratio. Under realistic conditions, confusion will become more severe as one pushes to smaller systems near the sample detection threshold (Bahcall et al. 2003).

With the advantage of full spatial information, theorists working with simulated volumes are afforded higher precision. For a point set of simulation particles, percolation methods, such as the "friends-of-friends" algorithm of Davis et al. (1985), have been a popular way to

define halos. Complex geometries typically bound the objects defined with this method (see Fig. 4 of White 2001), and this aspect can complicate attempts to connect this mass measure to observations.

A geometrically simpler approach is to identify a cluster as material lying within a sphere, centered on a local density maximum or potential minimum, whose radial extent r_Δ is defined by an enclosed isodensity condition $M(< r_\Delta)/(4\pi {r_\Delta}^3/3) = \rho_t(z)$. Such spherical overdensity (SO) masses require a choice of threshold density $\rho_t(z)$ that is typically written as a multiple Δ of either the mean mass density $\rho_m(z)$ or the critical density $\rho_c(z)$. These measures are referred to as "mean" and "critical" masses below. Although many treatments employ a time-varying Δ in cosmologies with $\Omega_m \neq 1$ (Eke, Cole, & Frenk 1996), evidence below suggests that this complication is unnecessary, and Δ here is assumed constant.

Given a mass measure M, the space density $n(M,z|\mathcal{C})$, or *mass function*, describes the probability of finding a cluster at redshift z with total mass in the interval M to $Me^{d\ln M}$ within a suitably small comoving volume element dV:

$$p(M,z|\mathcal{C}) \;=\; n(M,z|\mathcal{C})\,dV. \tag{1.5}$$

An analytic form for the mass function, based on spherical dynamics and a Gaussian random density field, was first developed by Press & Schechter (1974, hereafter PS) and rederived using a rigorous excursion set approach by Bond et al. (1991). The resulting shape of $n(M,z)$ is dictated by the linear power spectrum $\sigma(M)$ and its logarithmic derivative. The mass fraction in halos of mass M at redshift z can be expressed in terms of a single function $f(\sigma^{-1})$:*

$$f(\sigma^{-1},z) \;\equiv\; \frac{M}{\rho_m(z)}\, n(M,z)\, \frac{d\ln M}{d\ln \sigma^{-1}}. \tag{1.6}$$

The dependence on cosmology is implicit, determined by the fluctuation spectrum and its rate of linear evolution $D(a)$.

The PS treatment employs a spherical collapse model that assumes equilibrium is reached when the linearly evolved interior density reaches a critical threshold δ_c (equal to 1.686 in an Einstein-de Sitter cosmology). This leads to a mass function of the form

$$f(\sigma^{-1}) \;=\; \sqrt{2/\pi}\,(\delta_c\sigma^{-1})\,\exp[-(\delta_c\sigma^{-1})^2/2]. \tag{1.7}$$

Initial comparison of the model with N-body simulations yielded good agreement (Efstathiou et al. 1988), but as computational dynamic range and fidelity improved, disagreement in the detailed shape of the mass function emerged. Introduction of ellipsoidal, rather than spherical, perturbation evolution greatly improved agreement with simulations (Sheth & Tormen 1999; Sheth, Mo, & Tormen 2001, hereafter ST). The mass function in this case takes the form

$$f(\sigma^{-1}) \;=\; A_{ST}\sqrt{2a/\pi}\,[1+(a\delta_c\sigma^{-1})^{-p}]\,(\delta_c\sigma^{-1})\,\exp[-(a\delta_c\sigma^{-1})^2/2], \tag{1.8}$$

with parameters $A_{ST} = 0.3222$, $a = 0.707$, and $p = 0.3$.

Massively parallel computers, with aggregate memory in excess of one terabyte, have enabled production of very large statistical samples of virtual clusters. Calibrations of the mass function from such samples are reported in a number of recent papers (Governato et al.

* Note that, since $\sigma(M)$ is a monotonic decreasing function in cold dark matter models, its inverse $\sigma^{-1}(M)$ has the same sense as mass; high σ^{-1} implies high mass and *vice versa*.

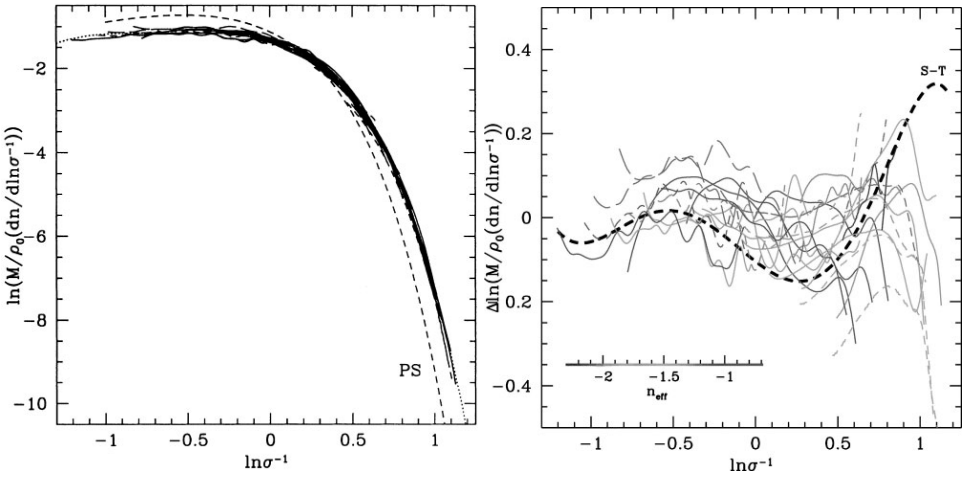

Fig. 1.2. Calibration of the mass function from a set of 29 halo samples extracted from Virgo Consortium simulations (Jenkins et al. 2001). *Left:* Mass fraction in halos as a function of the similarity variable $\sigma^{-1}(M)$. The dotted curve shows the fit to the Jenkins mass function (Eq. 1.9), while the dashed curve shows that the PS expectation (Eq. 1.7) has the wrong shape. *Right:* Residuals in number density between the binned simulated samples and the Jenkins mass function fit are shown as thin lines. The dashed line shows the difference between the Jenkins mass function and ST prediction (Eq. 1.8), with parameters given in the text.

1999; Bode et al. 2001; Jenkins et al. 2001; Evrard et al. 2002; Hu & Kratsov 2003; Reed et al. 2003). The results from analysis of a suite of simulations performed by the Virgo Consortium (Jenkins et al. 2001) are shown in Figure 1.2. The mass fraction as a function of $\sigma^{-1}(M)$ is shown for 29 halo samples identified in 13 simulations and covering epochs $z \approx 0-5$ in four different cosmological models (see Table 2 of Jenkins et al. 2001).

All of the models are well fit by a function (hereafter the Jenkins mass function) of the form

$$f(\ln \sigma^{-1}) \;=\; A\, \exp[-|\ln \sigma^{-1} + B|^{\epsilon}]. \tag{1.9}$$

The parameter B controls the location of the peak in the collapsed mass fraction (e^B plays the role of δ_c in the PS and ST forms) while A controls the overall mass fraction in halos and ϵ stretches the function to fit the overall shape of the simulation results. Values $A=0.315$, $B=0.61$, and $\epsilon=3.8$ fit the data in Figure 1.2, which uses a friends-of-friends mass measure with a linking length of 0.2 times the mean interparticle spacing. Note that these parameters are independent of cosmological model and epoch. In this sense, it may be said that Nature prefers to do *accounting* relative to the mean mass density.

We will see below that Nature appears to prefer doing *dynamics* relative to the critical density. For a critical SO(200) mass measure, Evrard et al. (2002) show that Equation (1.9) provides a good fit to the mass function with Ω_m-dependent fit parameters $A(\Omega_m)=0.27-0.07\Omega_m$ and $B(\Omega_m)=0.65+0.11\Omega_m$ (and $\epsilon=3.8$). Hu & Kravtsov (2003) provide independent confirmation of this fit for the case $\Omega_m=0.15$.

The right panel of Figure 1.2 shows that this form predicts the space density to an accu-

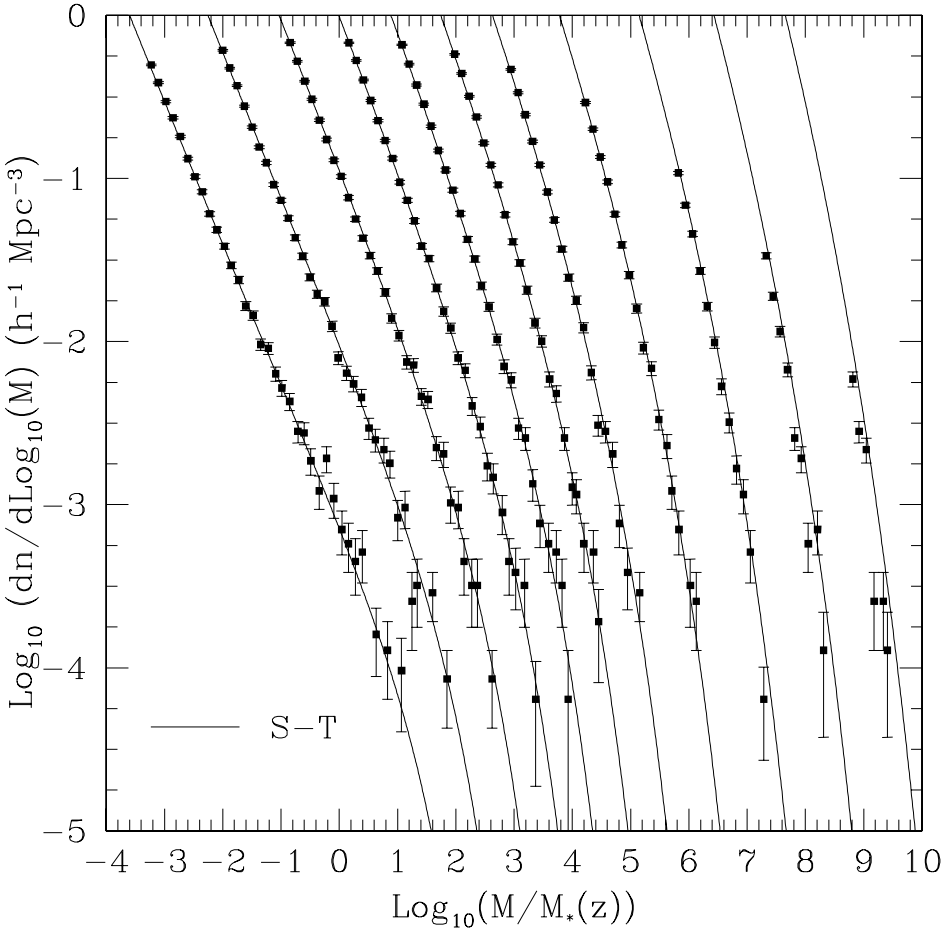

Fig. 1.3. The mass function of halos from the ΛCDM simulation of Reed et al. (2003). Data points with Poisson error bars show the simulation results, while curves are ST predictions at redshifts (from left to right) 0, 1, 2, 3, 4, 5, 6.2, 7.8, 10, 12.1, and 14.5.

racy of $\sim 20\%$. This panel also shows deviations with respect to the ST form with recalibrated parameters $A_{\rm ST} = 0.353$, $a = 0.73$, and $p = 0.175$. With the exception of the rarest objects ($\ln \sigma^{-1} \gtrsim 0.7$), this model gives an equally good fit. The PS formula for the rarest systems underpredicts their abundance by more than a factor 10. The use of an ellipsoidal collapse model (with two added parameters calibrated by simulation) is clearly superior to the original PS spherical treatment.

Reed et al. (2003) reach a similar conclusion on the ST predictions, and offer a correction factor to apply at high masses. As shown in Figure 1.3, their 432^3 particle simulation of a $50\,h^{-1}$ Mpc region, which probes a more shallow region of the power spectrum compared to cluster scales, shows stunning agreement with the ST predictions over a wide dynamic

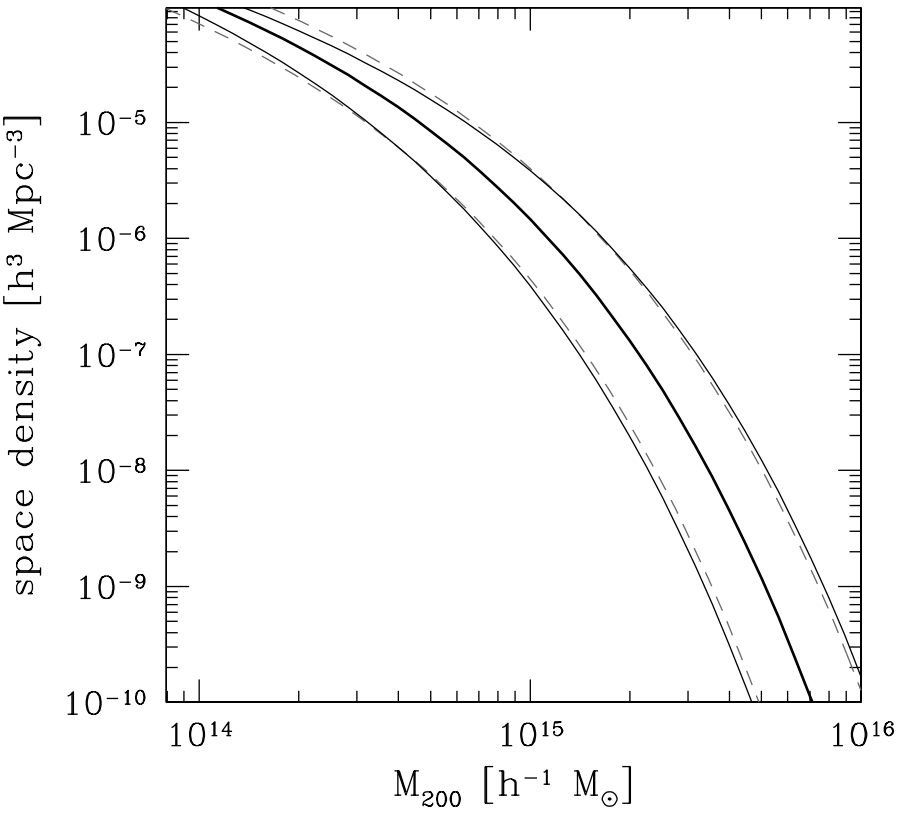

Fig. 1.4. The bold line shows the Jenkins mass function expectations for a ΛCDM cosmology with a default value $\sigma_8 = 0.9$. Solid lines to the right and left of the default give the Jenkins mass function for modified normalizations $\sigma_8 = 0.9\, e^{\pm 0.148}$. The dashed lines show the default Jenkins mass function with masses displaced by amounts $e^{\pm 0.371}$. The degeneracy between mass scale and σ_8 is apparent at space densities below $10^{-5} h^3$ Mpc^{-3}.

range in number density and epoch. The finding that the fit works well over 10 decades in normalized mass $M/M_*(z)$ is particularly impressive.

1.2.3 Mass-scale Uncertainty and σ_8

The space density of the most massive clusters at a given epoch is exponentially sensitive to σ_8, but extracting σ_8 from observations of massive clusters requires accurate knowledge of cluster masses. From the form of the Jenkins mass function, Evrard et al. (2002) derive $\mathrm{d}\ln\sigma_8/\mathrm{d}\ln M \simeq 0.4$ for massive clusters in a ΛCDM cosmology, meaning that, at fixed spatial abundance, systematic errors of, say, 25% in the mass scale of clusters translate into a systematic uncertainty of 10% in σ_8. A simple demonstration of this effect is given in Figure 1.4. The shapes of the functions, scaled separately in mass or σ_8, are nearly identical over the space density range 10^{-5} to $10^{-10} h^3$ Mpc^{-3}.

In summary, computational modeling now provides $\sim$10%-level accurate calibration of